IJAO
ISSN 0391-3988

Int J Artif Organs 2017; 40(7): 350-357
DOI: 10.5301/ijao.5000598

ORIGINAL RESEARCH ARTICLE

Open Access

Biostable scaffolds of polyacrylate polymers implanted in the articular cartilage induce hyaline-like cartilage regeneration in rabbits

María Sancho-Tello[1,2], Francisco Forriol[2,3], José J. Martín de Llano[1,2], Carmen Antolinos-Turpin[2,4], José A. Gómez-Tejedor[4,5], José L. Gómez Ribelles[4,5], Carmen Carda[1,2,5]

[1] Department of Pathology, Faculty of Medicine and Odontology, University of Valencia, Valencia - Spain
[2] INCLIVA Biomedical Research Institute, Valencia - Spain
[3] Hospital de la Malvarrosa, Valencia - Spain
[4] Centre for Biomaterials and Tissue Engineering, Polytechnic University of Valencia, Valencia - Spain
[5] Biomedical Research Networking Center on Bioengineering, Biomaterials and Nanomedicine (CIBER-BBN), Valencia - Spain

ABSTRACT

Purpose: To study the influence of scaffold properties on the organization of in vivo cartilage regeneration. Our hypothesis was that stress transmission to the cells seeded inside the pores of the scaffold or surrounding it, which is highly dependent on the scaffold properties, determines the differentiation of both mesenchymal cells and dedifferentiated autologous chondrocytes.

Methods: 4 series of porous scaffolds made of different polyacrylate polymers, previously seeded with cultured rabbit chondrocytes or without cells, were implanted in cartilage defects in rabbits. Subchondral bone was injured during the surgery to allow blood to reach the implantation site and fill the scaffold pores.

Results: At 3 months after implantation, excellent tissue regeneration was obtained, with a well-organized layer of hyaline-like cartilage at the condylar surface in most cases of the hydrophobic or slightly hydrophilic series. The most hydrophilic material induced the poorest regeneration. However, no statistically significant difference was observed between preseeded and non-preseeded scaffolds. All of the materials used were biocompatible, biostable polymers, so, in contrast to some other studies, our results were not perturbed by possible effects attributable to material degradation products or to the loss of scaffold mechanical properties over time due to degradation.

Conclusions: Cartilage regeneration depends mainly on the properties of the scaffold, such as stiffness and hydrophilicity, whereas little difference was observed between preseeded and non-preseeded scaffolds.

Keywords: Animal models, Biopolymers, Cartilage, Scaffolds, Tissue engineering

Introduction

Articular cartilage has a very limited ability to repair itself (1); thus, traumatic injuries, osteochondritis dissecans, and degenerative processes lead to severe cartilage lesions, eventually accompanied by pain, immobility, stiffness, and progressive joint destruction. Different therapeutic strategies have been developed to prevent their progression, including tissue-response techniques, such as drilling (2), microfracture (3), osteochondral transplantation (4), and the transplantation of periosteum or perichondrium to resurface damaged cartilage (1, 5). The results of these techniques are not always satisfactory, and thus microfracture-treated superficial defects remain unhealed (6), while full-depth defects may heal with fibrocartilaginous tissue by recruiting mesenchymal stem cells from the subchondral bone marrow (6, 7).

Human autologous chondrocyte transplantation (8) has been used successfully and is considered the gold standard in the repair of osteochondral injuries. However, its major disadvantages include a wide arthrotomy incision, the need to obtain enough cells for large defects, and the fact that patients need to undergo 2 surgeries (7).

Tissue engineering techniques are leading to promising results in articular cartilage regeneration (9), using empty scaffolds or those seeded with autologous chondrocytes (10, 11). Scaffolds play important roles because they rapidly fill

Accepted: April 12, 2017
Published online: May 24, 2017

Corresponding authors:
María Sancho-Tello, MD, PhD
Departamento de Patología
Facultad de Medicina y Odontología
Universitat de València
Av. Blasco Ibáñez 15
E-46010 Valencia, Spain
stello@uv.es

TABLE I - Number of animals used per treatment group and compressive strength measurement of the scaffolds of the different series

Series	Composition	Number of animals		*E* (MPa)
		Non-preseeded	Preseeded	
I	P(EA-co-MAAc) 90/10	2	2	1.48 ± 0.64
II	P(EA-co-HEA) 90/10	8	5	0.57 ± 0.10
III	P(EA-co-HEA) 50/50	2	2	0.20 ± 0.03
IV	PEA 100	8	5	2.24 ± 0.73
Control		4	-	-

Values are mean ± standard deviation of the Young's modulus (MPa).

cartilage defects, provide a substrate where cells can adhere, and maintain mechanical integrity, withstanding mechanical stresses. Thus, they should be designed to match the mechanical properties of native cartilage and support joint loading conditions (9, 12, 13).

Our aim was to compare in vivo cartilage regeneration by implanting scaffolds made of biostable materials of similar composition but with varying compliance, preseeded with chondrocytes or not, using a series of polyacrylate polymer and copolymer networks, previously used in in vitro studies on cell adhesion and viability (14-18). In contrast to other studies (11, 19, 20), the materials we used were biocompatible, biostable polymers; thus, our results are not affected by any effect attributable to material degradation products or to loss of mechanical properties over time due to scaffold degradation.

Methods

Polymeric scaffolds

Macroporous scaffolds were made of polymer or copolymer networks (Tab. I): copolymers of ethyl acrylate (EA) and 10% methacrylic acid (MAAc) [P(EA-co-MAAc)] (series I), copolymers of EA and hydroxyethyl acrylate (HEA) [P(EA-co-HEA)], containing 10% (series II) or 50% (series III) HEA, and poly(ethyl acrylate) (PEA; series IV). Triethyleneglycol dimethacrylate 5% (98%; Aldrich) was used as a cross-linking agent and 1% benzoin (Scharlau) as an ultraviolet photosensitive initiator.

Poly(methyl methacrylate) microspheres (PMMA; 90 µm average diameter; Colacryl DP300; Lucite International) were used as scaffold templates, sintered under pressure above its glass transition temperature (15). After polymerization, templates were dissolved with acetone for ~48 hours in a Soxhlet extractor, immersed in a large excess of acetone, and slowly changed to water to avoid scaffold collapse. Scaffold replicas were cut (~3 mm diameter, 1 mm thick), dried in vacuo for 24 hours at room temperature (RT), followed by 24 hours at 50°C, and sterilized with γ radiation (25 kGy) before use.

Series I and II scaffolds were slightly hydrophilic (bulk polymers could absorb 2.3% and 3.3% of their weight in water, respectively, measured on a dry basis when immersed in liquid water until equilibrium). Series III were hydrogels where the equilibrium water content was 18.1% by weight (16). Series IV scaffolds were hydrophobic. The volume fraction of scaffold pores was 0.75 ± 0.03 in all samples. Scaffold morphology was examined by scanning electron microscopy (SEM; JEOL-JSM6300) (10).

Mechanical properties of the scaffold

The compressive strength of the scaffold was measured in a thermo-mechanical analyzer (TMA-EXSTAR6000; Seiko Instruments) in control position mode with a 0.5-mm-diameter stainless steel probe (10). Cylindrical shape samples, 3.5 mm in diameter and 0.7 mm thick, were used for testing mechanical properties. Briefly, an initial 2% strain was applied for 15 minutes; subsequently, 4 programs of compression loading up to 15% strain and unloading were performed at RT, both at a 20 µm/min rate. Young's modulus was calculated from the slope of stress-strain curves in the linear region of the compression curve. Results are expressed as the average value ± standard deviation (SD) of a minimum of 5 measurements. For statistical analyses, we used R software (ver. 3.3.2).

Animals

In total, 38 adult male New-Zealand rabbits, weighing ~1.5 kg, were obtained from Granjas San Bernardo (Tulebra). They were quarantined for 7 days. Animals were housed in standard single cages under conventional conditions with appropriate bedding, controlled temperature and light, and provided free access to drinking water and food. The study protocol was approved by the ethics committee of the University of Valencia.

Rabbit chondrocyte harvesting and culture

To isolate chondrocytes, articular cartilage was obtained from knee joints of donor rabbits after their sacrifice with a lethal intravenous injection of 500 mg of thiopental (Tiobarbital; Braun) (10, 14). Briefly, cartilage was diced and successively incubated in enzymatic solutions. Isolated cells were diluted in Dulbecco's modified Eagle's medium (DMEM), supplemented with 10% fetal bovine serum (Invitrogen)

and 50 µg/mL ascorbic acid (Sigma-Aldrich), plated at high density, and cultured at 37°C in a 5% CO_2 humidified atmosphere (14).

Scaffolds were placed in a 24-well polystyrene culture plate, moistened with Hanks' balanced salt solution (Sigma-Aldrich), and cell suspension (10^6 viable cells/20 µL of medium) was injected in the center of the scaffolds to allow cells to infiltrate the porous structure. After 1 hour of incubation, scaffolds were changed to a new well and culture medium was gently added. After 3 days in culture, medium was replaced with DMEM containing 1% insulin-transferrin-sodium-selenite media supplement (BD Biosciences) and 50 µg/mL ascorbic acid, and scaffolds were cultured for 3 more days before implantation (10, 20).

Scaffold implantation

Scaffolds were implanted as described previously (10). Briefly, rabbits were preanesthetized by subcutaneous injection of 15 mg/kg ketamine (Ketolar; Pfizer) and intramuscular injection of 0.1 mg/kg medetomidine (Domtor, Pfizer). General anesthesia was induced with 4% isoflurane and maintained with 1.5% isoflurane with O_2 (2 L/min). Non-preseeded scaffolds were moistened with phosphate-buffered saline (PBS), and vacuum was applied to ensure liquid penetration into the pores.

Knee joint arthrotomy was performed through a parapatellar incision and the patella laterally dislocated. A 3-mm trephine was used to create a chondral defect (3 mm diameter, 1 mm depth) in the central articulating surface of the femoral trochlear groove, injuring the subchondral bone, allowing blood to flow towards the injury site. After rinsing with sterile saline, a scaffold was laid into the defect and held in place by repositioning the patella. The arthrotomy and skin were sutured. After surgery, analgesia and antibiotic prophylaxis was administered and rabbits were returned to their cages and allowed free cage activity. Control animals received the same surgical procedure, including the 3-mm defect in the trochlea, but no scaffold was implanted.

The results observed after a first batch of animals (n = 2 animals/group) were not satisfactory in series I or III. Thus, no additional animals were employed for these series, and only the numbers of animals in series II, IV, and controls were increased. The total numbers of animals/group are detailed in Table I.

Animal sacrifice and tissue retrieval

After surgery, the rabbits showed good general states, with no osteoarticular complication or infection, and normal activity. At 3 months after surgery, rabbits were sacrificed, as described above. The knee articular surface was observed and macroscopic pictures were taken.

Histological studies

Morphology was studied following standard histological procedures (10, 11). Briefly, articular specimens were fixed (4% formaldehyde, 5 days) and immersed in Osteosoft decalcifier solution (Merck) for 5 to 8 weeks. Then, samples were embedded in paraffin, 5-µm-thick serial sections were obtained in the middle part of the scaffolds (~3 mm diameter), and stained with hematoxylin-eosin and Masson's trichrome. The presence of chondral glycosaminoglycan was monitored by Alcian blue staining (pH 2.5) and counterstained with Harris hematoxylin. Sections were analyzed under a Leica-DM4000B optical microscope, and pictures were taken using a camera (Leica-DFC420). Cell density (number of cells/mm^2) was quantified inside the implanted scaffolds as well as the distance between articular surface and scaffold, using Image proPlus 7.0 (Media Cybernetics). Results are expressed as average values ± SD of 4 measurements. Results were compared using Mann-Whitney *U*-test, and were considered statistically significant when the p value was <0.05. The square of the Pearson correlation coefficient (R^2) was used to determine the degree of linear regression between the parameters studied.

Results

Scaffolds were covered by neocartilage at 3 months after implantation in most cases, with neotissue occupying scaffold pores in both preseeded and non-preseeded samples. However, the quality of the neotissue depended on the nature of the material implanted rather than on the presence or absence of preseeded chondrocytes.

Figure 1A shows a representative scaffold observed with SEM, with a highly porous structure, which was studied in all series at higher magnification (Fig. 1B-E), showing spherical, interconnected pores with an average diameter around 60 µm, slightly smaller than the PMMA microspheres used as a template (90 µm), without significant differences between samples. Pores presented an elliptical shape in P(EA-co-HEA) copolymers (Fig. 1C, D), probably due to a certain degree of scaffold collapse during solvent exchange from acetone to water during template extraction. Although pores were well interconnected in all series, throat size between pores was slightly smaller in series I (Fig. 1B).

Scaffold Young's modulus values showed the highest stiffness corresponding to pure PEA scaffold (Tab. I). Copolymers containing HEA hydrophilic monomeric units presented a decreasing elastic modulus with increasing HEA content (series II and III), as expected. In contrast, scaffolds made of copolymers containing MMAc, which also provided a degree of hydrophilicity, had a stiffness close to that of pure PEA. This was ascribed to the methyl group attached to MMAc, which imposes a high energy barrier to the rotation of the main copolymer chain in P(EA-co-MMAc), thus tending to increase stiffness and balancing the effect of water sorption. The differences in Young's moduli between the different series were statistically significant ($p<0.05$), except between samples I and IV.

Macroscopic observation at the implant zone after sacrifice revealed that scaffolds were smoothly covered by a thin translucent tissue with apparently good integration into the osteoarticular complex. However, a different aspect than the adjacent native cartilage was observed in all series, with a whiter colour and a well-defined border (Fig. 2).

Microscopic analysis showed scaffold preservation 3 months after implantation (Fig. 3), observed as white spaces in series

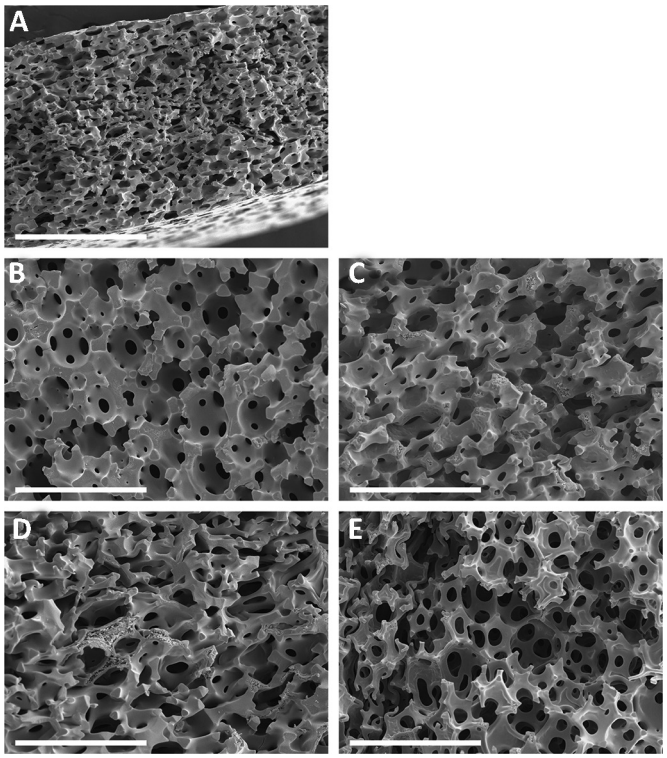

Fig. 1 - Scanning electron microscopy (SEM) of the scaffolds. (**A**) SEM cross-sectional image of P(EA-co-HEA) 50/50 (series III) scaffold. SEM pore structure images for all series: (**B**) series I, P(EA-co-MAAc) 90/10; (**C**) series II, P(EA-co-HEA) 90/10; (**D**) series III, P(EA-co-HEA) 50/50; and (**E**) series IV, PEA 100. Scale bars represent 500 µm (A) or 200 µm (B-E).

I, II, and IV, and slightly stained in series III, probably due to their hydrophilic properties. Neotissue had grown over most scaffolds as well as inside scaffold pores, except in series III. However, no statistically significant difference ($p>0.05$) was observed in cell density inside scaffolds when non-preseeded and preseeded scaffolds of each series were compared.

Series I had a mild, irregular response (Fig. 3A, E), with a neosynthesized superficial cartilage covering most of the scaffold surface; some samples were located away from the surface, whereas others were near it and presented areas in direct contact with the articular cavity (Fig. 4A), with a mean distance of 665 ± 387 µm. This material induced irregular scaffold integration within the osteoarticular complex, with some well-integrated zones, while other areas were surrounded by fibrous tissue. Colonization by neotissue was mild in non-preseeded samples and increased in preseeded ones (109 ± 44 cells/mm^2 vs. 289 ± 135 cells/mm^2, respectively, with no statistically significant difference).

Series II induced the best response (Fig. 3B, F), with a regenerated articular surface resembling hyaline cartilage in all samples (Fig. 4B). They showed good integration in the osteoarticular complex (Fig. 4B-D), although small areas surrounded by connective tissue were eventually observed. Scaffold pores were densely populated by neotissue in both non-preseeded and preseeded ones (271 ± 207 cells/mm^2 vs. 218 ± 164 cells/mm^2, respectively, with no statistically significant difference), with avascular hyaline-like cartilage occupying the upper and middle parts of the scaffolds (Fig. 4C), whereas in the lower part, it resembled bone tissue, containing mesenchymal and osteoblast-like cells along with blood vessels (Fig. 4D). Scaffolds were located at 951 ± 494 µm from the articular surface.

Series III showed the worst response (Fig. 3C, G). Superficial cartilage neoformation was mild in some samples but showed areas of fibrosis. Abundant dense fibrous tissue surrounded and frequently invaded all scaffolds, containing numerous giant multinucleated phagocytic cells (Fig. 4E). Moreover, neotissue formation inside the scaffolds was almost absent in both preseeded and non-preseeded samples (12 ± 25 cells/mm^2 vs. 18 ± 21 cells/mm^2, respectively, with no statistically significant difference). Scaffolds were located at a similar depth to those of series II (1088 ± 611 µm).

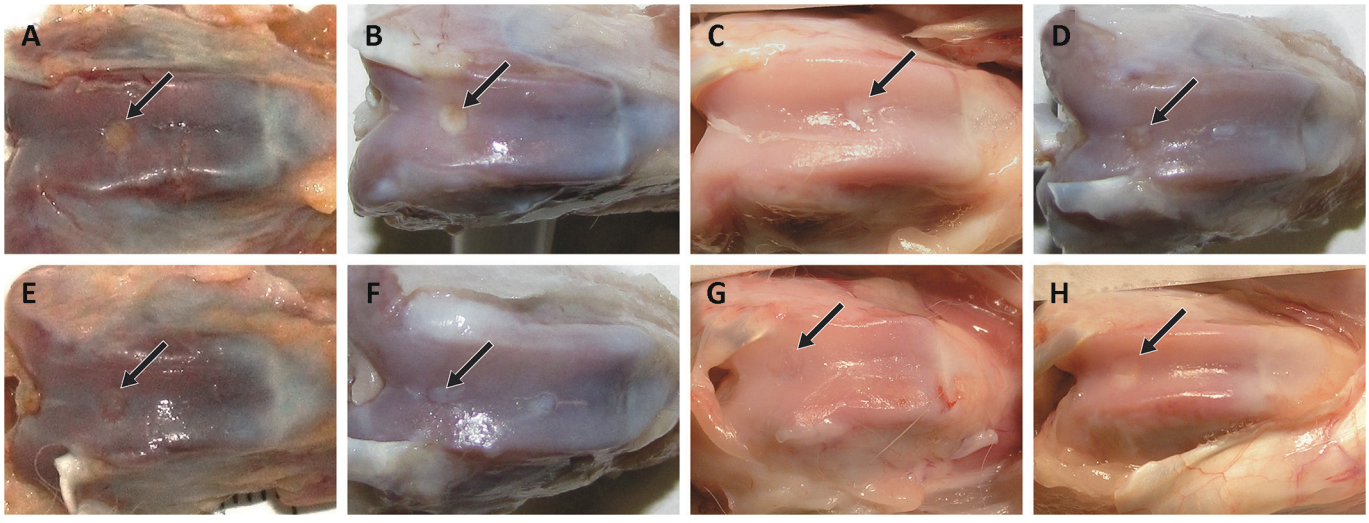

Fig. 2 - Representative macroscopic views of the articular surface of the different series, 3 months after scaffold implantation. **Arrows** show the injury zone of non-preseeded (**A**-**D**) or preseeded (**E**-**H**) series I to IV, respectively.

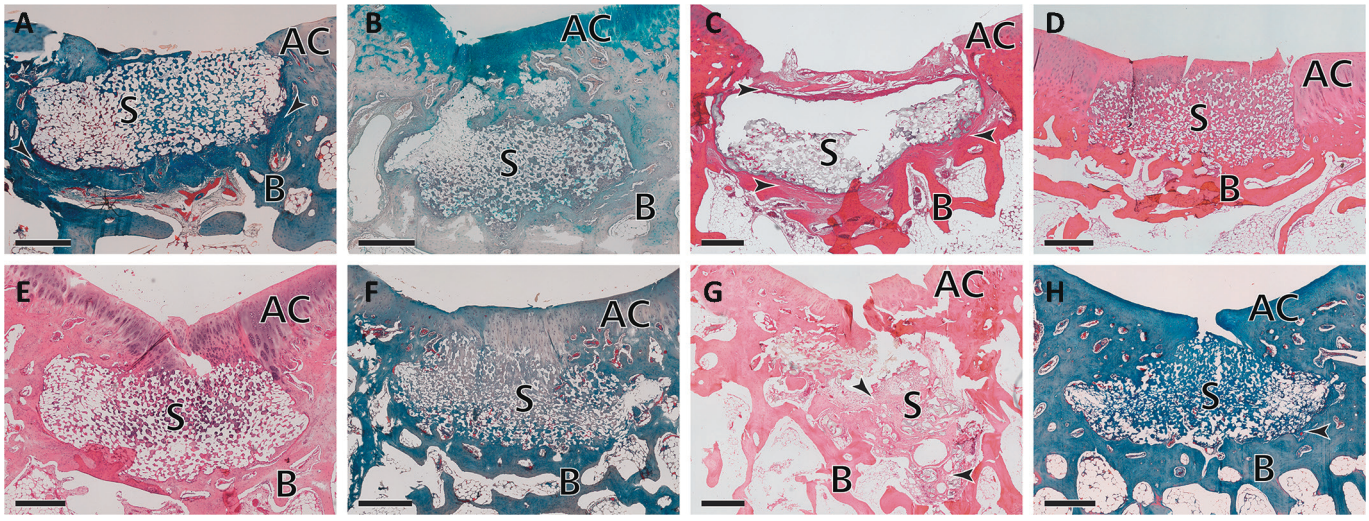

Fig. 3 - Representative microscopic panoramic views of implanted scaffolds of non-preseeded (**A**-**D**) or preseeded (**E**-**H**) series I to IV, respectively, 3 months after implantation. Series I, II, and IV biomaterials were not stained and thus appeared as white spaces, while series III material appeared slightly stained gray (**C**, **G**). Sections were stained with Masson's trichrome (**A**, **F**, **H**), Alcian blue (**B**), or hematoxylin-eosin (**C**, **D**, **E**, **G**). **Arrowheads** show fibrous tissue. AC = articular cartilage; B = subchondral bone; S = scaffold. Scale bars represent 500 µm.

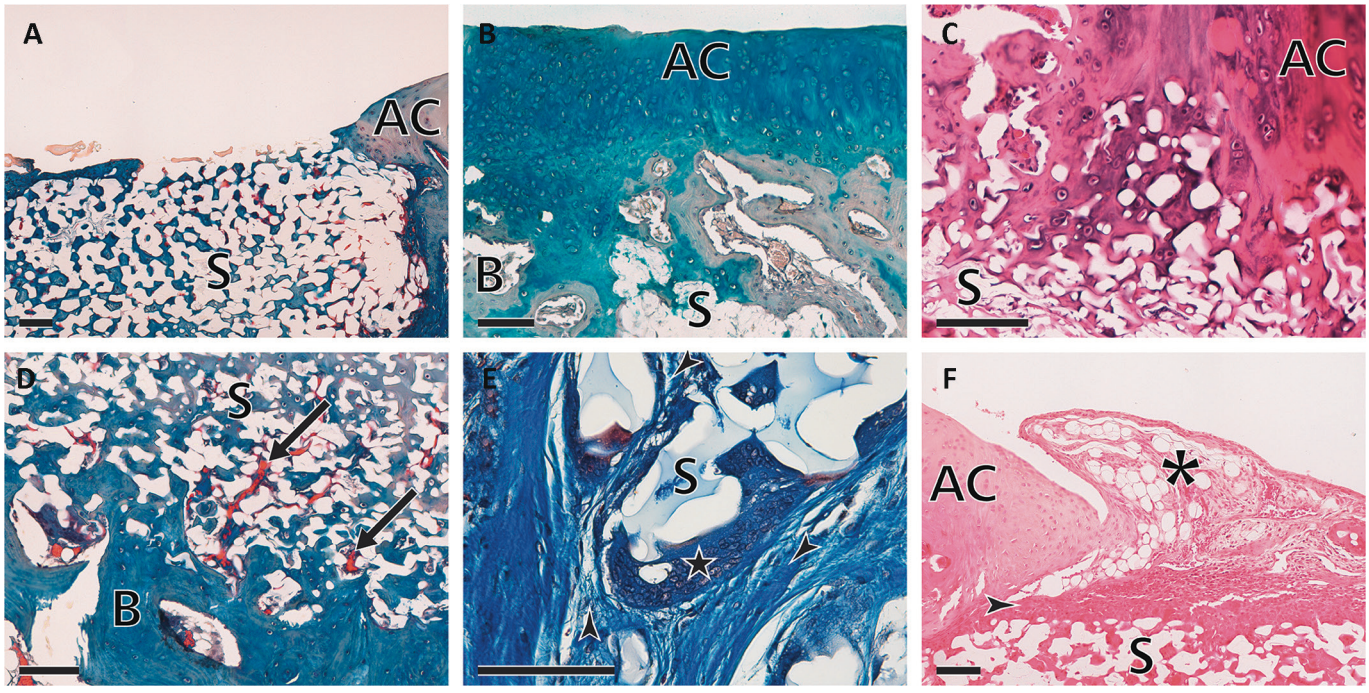

Fig. 4 - Different tissue responses to the implanted scaffolds, 3 months after implantation. (**A**) Non-preseeded scaffold series I contacts with the articular cavity. (**B**) Hyaline-like neocartilage grown on the surface of non-preseeded scaffold series II in continuity with native cartilage. (**C**) Good continuity between neocartilage grown within scaffold pores and surrounding superficial cartilage in preseeded series II. (**D**) Blood vessels (**arrows**) emerging from spongy bone tissue as well as good continuity between neotissue and subchondral bone in preseeded scaffold series II. (**E**) Abundant fibrous tissue (**arrowheads**) with numerous giant multinuclear phagocytic cells (**star**) inside and around the implanted preseeded scaffold series III, where the biomaterial is stained gray (S). (**F**) Synovial-like tissue (asterisk) over the implanted scaffold in non-preseeded series IV. Sections were stained with Masson's trichrome (**A**, **D**, **E**), Alcian blue (**B**), or hematoxylin-eosin (**C**, **F**). AC = articular cartilage; B = subchondral bone; S = scaffold. Scale bars represent 100 µm.

Series IV also showed a good response (Fig. 3D, H), although the reparative response at the surface seemed slower than in series II. Scaffolds were often close to the articular surface (in 8 of 13 samples), and some presented areas in direct contact with the cavity and eventually synovial-like tissue (Fig. 4F), as was also observed in some series I and III samples. Although a tendency of a closer location of the scaffold to the articular surface was observed in series

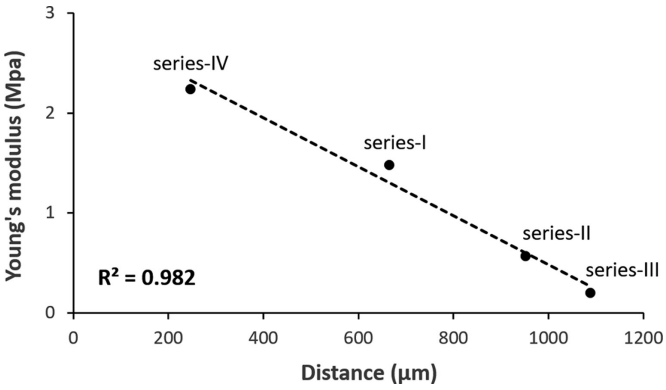

Fig. 5 - Linear regression between Young's modulus and scaffold distance from articular surface in the series studied. A high negative correlation coefficient (R^2) was observed.

IV (247 ± 190 µm) with respect to other series, no statistically significant difference was found ($p>0.05$). However, a high coefficient for a negative correlation was observed ($R^2 = 0.982$) when Young's modulus was plotted against the scaffold distance to the articular surface (Fig. 5). Series IV showed good integration with the osteoarticular complex although small areas of fibrosis surrounding scaffolds were also present. Neotissue grown inside scaffold pores was abundant in both non-preseeded and preseeded samples (445 ± 160 cells/mm^2 vs. 330 ± 234 cells/mm^2, respectively, with no statistically significant difference), with a similar morphological pattern to series II (cartilage in the top, bone tissue in the bottom).

Finally, control animals (Fig. 6), which underwent the same surgical procedure but where no scaffold was implanted, showed neotissue filling the chondral defect with macroscopic characteristics similar to those with scaffolds. However, microscopic analysis revealed the presence of fibrous tissue covering the whole defect.

Discussion

We showed in a previous study (10) that implanting a scaffold made of P(EA-co-HEA), series II, in a rabbit knee model, yielded the formation of hyaline cartilage, and thus the aim in this work was to determine the effect of scaffold compliance on tissue regeneration by increasing stiffness by substituting the hydrophilic component, HEA, by MAAc (series I) or by PEA (series IV), or on the contrary increasing compliance by increasing the HEA content (series III). We observed that cartilage-like neotissue covered scaffolds 3 months after implantation, and also that neotissue occupied scaffold pores in both preseeded and non-preseeded samples, but the quality of the neotissue depended on the nature of the material implanted. Implantation was accompanied by blood flow at the injury zone because we wounded the subchondral bone. Because no statistically significant difference was found between neotissue growth inside scaffolds in preseeded and non-preseeded scaffolds, our results suggest that neotissue originated primarily from the differentiation of mesenchymal cells that invaded the scaffold, whereas native cartilage around the lesion also participated in the neoformation of articular cartilage, that actively proliferated, as reported in a 1-year evolution study using series II scaffolds (10). When non-preseeded scaffolds were implanted, they immediately absorbed blood, even the most hydrophobic material (PEA), because their pores were filled with PBS before implantation. It is worth remarking that the scaffolds occupied the defect tightly and they were level with the surrounding condylar surface.

The behavior of invading cells and the tissue characteristics they generated depended on the scaffold properties. It is known that mesenchymal cells, recruited from subchondral bone marrow in microfracture-treated cartilage full defects (3), acquire a chondrogenic phenotype and produce cartilaginous extracellular matrix (ECM), which frequently degenerates into fibrocartilage (5). Our innovation was that we filled the defect with a polymeric scaffold, modifying the mechanical loading state to which cells were subjected, showing the important effect of biomechanics (9, 20, 21) at the defect site during regeneration on the neotissue quality, also favoring lateral integration (7). If subchondral bone is microfractured but the defect site is kept empty, a layer of cartilage is formed 3 months after implantation, but regenerated tissue does not fully occupy the defect site (20). The cells located at the defect site are not subjected to compression loading, which is withstood by the noninjured surrounding cartilage. However,

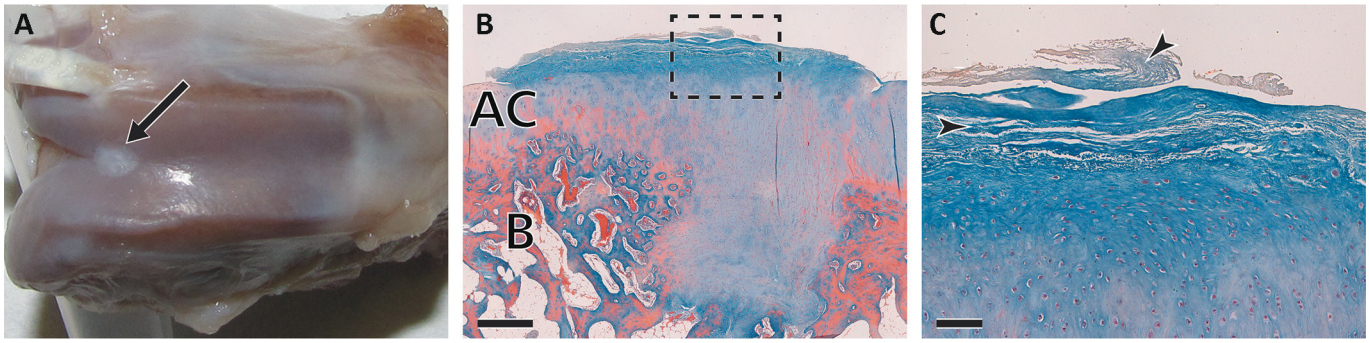

Fig. 6 - Control samples. Representative macroscopic view of the articular surfaces (**A**) and microscopic views (**B**, inset **C**), 3 months after surgery. Sections were stained with Masson's trichrome (**B**, **C**). **Arrow** shows the injury zone and **arrowhead** fibrous tissue. AC = articular cartilage; B = subchondral bone. Scale bars represent 500 µm (B) or 100 µm (C).

when scaffolds filled the defect site, cells located at the condylar surface over the scaffold were subjected to compressive stresses and reacted by producing cartilaginous ECM.

The neotissue generated had hyaline-like cartilage characteristics: isolated cells in lacunae forming perpendicular columns to the surface, and a cartilaginous ECM. Obviously, the biomechanics at the surface is highly dependent on the material elastic modulus, and in our scaffolds, Young's modulus was similar to those reported for cartilage in rabbits (20) (0.41 ± 0.12 MPa) and humans (22) (0.58 ± 0.17 MPa). Moreover, mesenchymal cells that invaded the scaffold porous structure and produced ECM continuously increased the elastic modulus of the scaffold-cell construct. However, the ability to grow in the depth of the regenerated superficial cartilage depends on scaffold deformability. In control samples, where no scaffold was implanted and thus no compressive stresses were transmitted to surrounding tissue, a highly fibrous neotissue was observed filling and covering the excavated lesion, as observed previously (10, 20).

Implant location 3 months after surgery seemed to be the result of a competition between two forces: the growth in depth of regenerated cartilage on top of the material, which deformed the scaffold and pushed it downward, and the increased resistance of the scaffold bulk itself due to the regenerated tissue in its pores (10). This may explain the different scaffold locations observed as a function of the material elasticity, and actually we saw a high negative correlation when Young's modulus was plotted against scaffold distance from the articular surface. Thus, PEA, the stiffest material, seemed unaltered from its original location and showed the thinnest layer of hyaline cartilage on top, while the hydrogel P(EA-co-HEA)50/50, much softer due to its hydrophilicity, was often deformed and compressed in the subchondral bone. This latter material not only lacked regenerated tissue within its pores, but also induced a highly reactive fibrosis around it. The behavior of series I and II scaffolds, of average stiffness, was intermediate, with a thick layer of hyaline cartilage covering the scaffold.

The biological response also depended on the scaffold chemical composition. Thus, the P(EA-co-MAAc) copolymer contains acid groups in the MAAc unit that dissociate in aqueous medium, leaving negative electrical charges attached to the polymer chain, which was favorable for several cell types in vitro (16-18), but the in vivo response was poor because only mild colonization was observed along with fibrotic areas partly surrounding both preseeded and non-preseeded scaffolds.

The P(EA-co-HEA) copolymers contain hydroxyl groups in the side chains of the polymer backbone that increase water absorption capacity and diminish in vitro cell attachment (14, 16, 17), which did not correlate with the in vivo response. Thus, series II and IV, which showed the best performance, had scaffold pores filled with abundant cells isolated in lacunae. We previously showed the presence of proliferative cells in series II scaffolds (10). Given the poor proliferating nature of in vivo adult chondrocytes, these results suggest that cells colonizing the scaffolds came from the proliferation of both mesenchymal cells and preseeded chondrocytes. The scarcity of cells inside the P(EA-co-HEA) 50/50 scaffold could be due to the lack of cell attachment mentioned above and/or to the collapse of these soft scaffolds due to compressive forces exerted by the tissue growing on top of the surface that pushed the scaffold towards subchondral bone.

Morphological comparison of the regenerated tissue between non-preseeded and preseeded scaffolds showed similar general characteristics, but there was no statistically significant difference in cell density inside scaffolds in any of the series studied. The tissue that occupied scaffold pores resembled hyaline cartilage, with cells isolated in lacunae and an ECM containing specific cartilage components (10). In preseeded scaffolds, at least some of these cells probably originated from mesenchymal cells invading the scaffold, as discussed above, but the seeded dedifferentiated chondrocytes that were also able to result in in vivo hyaline-like tissue did not represent a significant difference.

Similarly, no significant difference was observed in the regenerated tissue over scaffold surfaces between preseeded and non-preseeded ones, suggesting that the regeneration mechanism is the same, and it depends essentially on the mechanical characteristics of the material rather than on the presence or absence of preseeded cells. In fact, when polycaprolactone scaffolds were used in a protocol similar to ours, but avoiding any injury of subchondral bone (therefore preventing blood flow at the implantation site), no top layer of hyaline cartilage was observed 3 months after implantation, although scaffold pores showed cartilaginous tissue (20).

Thus, hyaline-like cartilage was regenerated in rabbit articular defects 3 months after implanting porous scaffolds, and morphological differences were observed between the diverse series as a function of their stiffness and hydrophilicity. Good scaffold integration was observed in the host tissue, although scaffolds with lower stiffness appeared protruded towards subchondral bone and covered by an upper layer of hyaline-like tissue, whereas stiffer scaffolds were located mainly closer to the articular surface; the neotissue invading its pores was hyaline-like cartilage in the scaffold middle and upper parts, while bone-like tissue and ingrowth of vessels were observed in the lower part. These findings were similar in non-preseeded scaffolds and in those preseeded with in vitro expanded chondrocytes.

This suggests that the regenerated tissue originated mainly from the differentiation of mesenchymal cells that arrived from subchondral bone as a consequence of the surgical procedure, and differentiated towards a hyaline-like chondrocytic phenotype in a process strongly dependent on the transmission of mechanical stresses to the cells (20, 21). Thus, the critical role of the scaffold is to guarantee cell exposure to a mechanical environment capable of withstanding immediate compression forces and to transmit them to the cells from the very first moment after surgery, triggering their differentiation towards a chondrocytic lineage, which is important in the design of scaffolds for cartilage regeneration (12).

Conclusions

The regeneration of a smooth and functional joint surface is the consequence of the formation of a layer of hyaline-like cartilage on the surface of the scaffold. This seems to depend mainly on the mechanical properties of the scaffold that pro-

vides mesenchymal stem cells that invade the defect zone from subchondral bone with an adequate biomechanical environment, not only inside scaffold pores but also between the scaffold and the articular surface. Additional cellularity due to preseeding the scaffold with chondrocytes seems to play a minor role in the histology of the regenerated tissue and in the integration with surrounding tissues.

Acknowledgments

The authors are grateful to the Electronic Microscopy Service of the Polytechnic University of Valencia for its valuable help, to R. García Gómez for technical assistance in scaffold preparation, and to J. Benavent regarding histological techniques.

Disclosures

Financial support: Supported by the Ministry of Economy and Competitiveness through project No. MAT2013-46467-C4-R, including the FEDER financial support. CIBER-BBN is an initiative funded by the VI National R&D&I Plan 2008-2011, Iniciativa Ingenio 2010, Consolider Program. CIBER Actions are financed by the Instituto de Salud Carlos III with assistance from the European Regional Development Fund.
Conflict of interest: None of the authors has financial interest related to this study to disclose.

References

1. Nelson L, Fairclough J, Archer CW. Use of stem cells in the biological repair of articular cartilage. Expert Opin Biol Ther. 2010;10(1):43-55.
2. Insall J. The Pridie debridement operation for osteoarthritis of the knee. Clin Orthop Relat Res. 1974;101:61-67.
3. Steadman JR, Rodkey WG, Briggs KK, Rodrigo JJ. [The microfracture technic in the management of complete cartilage defects in the knee joint]. Orthopade. 1999;28(1):26-32 [Article in German].
4. Hangody L, Kish G, Kárpáti Z, Udvarhelyi I, Szigeti I, Bély M. Mosaicplasty for the treatment of articular cartilage defects: application in clinical practice. Orthopedics. 1998;21(7):751-756.
5. Minas T, Nehrer S. Current concepts in the treatment of articular cartilage defects. Orthopedics. 1997;20(6):525-538.
6. Steinwachs MR, Guggi T, Kreuz PC. Marrow stimulation techniques. Injury. 2008;39(Suppl 1):S26-S31.
7. Richter W. Mesenchymal stem cells and cartilage in situ regeneration. J Intern Med. 2009;266(4):390-405.
8. Brittberg M, Lindahl A, Nilsson A, Ohlsson C, Isaksson O, Peterson L. Treatment of deep cartilage defects in the knee with autologous chondrocyte transplantation. N Engl J Med. 1994;331(14): 889-895.
9. Ahmed TA, Hincke MT. Strategies for articular cartilage lesion repair and functional restoration. Tissue Eng Part B Rev. 2010;16(3):305-329.
10. Sancho-Tello M, Forriol F, Gastaldi P, et al. Time evolution of in vivo articular cartilage repair induced by bone marrow stimulation and scaffold implantation in rabbits. Int J Artif Organs. 2015;38(4):210-223.
11. Vikingsson L, Sancho-Tello M, Ruiz-Saurí A, et al. Implantation of a polycaprolactone scaffold with subchondral bone anchoring ameliorates nodules formation and other tissue alterations. Int J Artif Organs. 2015;38(12):659-666.
12. Little CJ, Bawolin NK, Chen X. Mechanical properties of natural cartilage and tissue-engineered constructs. Tissue Eng Part B Rev. 2011;17(4):213-227.
13. Vikingsson L, Gallego Ferrer G, Gómez-Tejedor JA, Gómez Ribelles JL. An in vitro experimental model to predict the mechanical behavior of macroporous scaffolds implanted in articular cartilage. J Mech Behav Biomed Mater. 2014;32:125-131.
14. Pérez Olmedilla M, Garcia-Giralt N, Pradas MM, et al. Response of human chondrocytes to a non-uniform distribution of hydrophilic domains on poly (ethyl acrylate-co-hydroxyethyl methacrylate) copolymers. Biomaterials. 2006;27(7):1003-1012.
15. Diego RB, Olmedilla MP, Aroca AS, et al. Acrylic scaffolds with interconnected spherical pores and controlled hydrophilicity for tissue engineering. J Mater Sci Mater Med. 2005;16(8): 693-698.
16. Campillo-Fernandez AJ, Pastor S, Abad-Collado M, et al. Future design of a new keratoprosthesis. Physical and biological analysis of polymeric substrates for epithelial cell growth. Biomacromolecules. 2007;8(8):2429-2436.
17. Campillo-Fernández AJ, Unger RE, Peters K, et al. Analysis of the biological response of endothelial and fibroblast cells cultured on synthetic scaffolds with various hydrophilic/hydrophobic ratios: influence of fibronectin adsorption and conformation. Tissue Eng Part A. 2009;15(6):1331-1341.
18. Soria JM, Sancho-Tello M, Esparza MA, et al. Biomaterials coated by dental pulp cells as substrate for neural stem cell differentiation. J Biomed Mater Res A. 2011;97A(1):85-92.
19. Izquierdo R, Garcia-Giralt N, Rodriguez MT, et al. Biodegradable PCL scaffolds with an interconnected spherical pore network for tissue engineering. J Biomed Mater Res A. 2008;85A(1): 25-35.
20. Martinez-Diaz S, Garcia-Giralt N, Lebourg M, et al. In vivo evaluation of 3-dimensional polycaprolactone scaffolds for cartilage repair in rabbits. Am J Sports Med. 2010;38(3):509-519.
21. Schulze-Tanzil G. Activation and dedifferentiation of chondrocytes: implications in cartilage injury and repair. Ann Anat. 2009;191(4):325-338.
22. Jurvelin JS, Buschmann MD, Hunziker EB. Mechanical anisotropy of the human knee articular cartilage in compression. Proc Inst Mech Eng H. 2003;217(3):215-219.